Probabilistic Loss Sensitivity Analysis in Power Distribution Systems

Mohammad Abujubbeh, *Student Member, IEEE*, Sai Munikoti, *Student Member, IEEE*, Anil Pahwa, *Fellow, IEEE*, and Balasubramaniam Natarajan, *Senior Member, IEEE*

***Abstract*—Power distribution systems are changing due to renewable energy integration, electric vehicle penetration and active consumers engaging in the energy market. Therefore, utilities need to quantify the impact of such changes on the system. Power loss is one of the tools to quantify system performance. A huge share of losses occurs on the distribution side due to lower voltages compared to transmission systems. Existing methods that quantify the impact of consumer activities on losses are scenario-specific, computationally expensive and do not consider uncertainties associated with power changes. Therefore, the goal of this paper is to develop a simpler, yet accurate, probabilistic loss sensitivity framework for approximating the impact of random power changes on power losses. First, an analytical expression is derived to approximate the change in line losses for any given deterministic power changes. Then, the analytical expression is extended to a probabilistic framework that accommodates variability related to power changes. The proposed approach is validated via simulation against the traditional load flow-based sensitivity method using the IEEE 69 node test system. Results demonstrate that the proposed approach is accurate and computationally efficient. The proposed framework is useful for real-time loss monitoring and optimal asset management.**

***Index Terms*—Active consumer, distribution system, sensitivity analysis, power loss, distributed energy resources**

I. Introduction

Power distribution systems across the globe are witnessing various structural changes as a response to the exponential growth in energy demand, increased impacts of climate change, and aging system infrastructure. There is growing investment in green distributed energy resources (DERs), e.g., rooftop solar photovoltaic (PV), for the numerous environmental, technical and, economic advantages they provide [1]. Yet, if not properly planned, DERs can also pose new technical challenges to system operation like increased power losses [2], nodal over-voltages [3], and reverse power flow [4]. These issues can result in economic losses and degradation of overall system efficiency. In this regard, the sensitivity of system losses to the changes in nodal complex power is perceived as a powerful tool that enables system planning [5]. For instance, loss sensitivity can be used for optimal DER [6] and capacitor [7] placement and sizing, feeder reconstruction and network configuration [8] or, optimal allocation of electric vehicle (EV) parking lots [9]. Therefore, the development of a generic method that studies the impact of DERs on system losses is a crucial aspect of modern distribution system planning and real-time monitoring.

Mohammad Abujubbeh, Sai Munikoti, Anil Pahwa, and Balasubramaniam Natarajan are with the Electrical and Computer Engineering Department, Kansas State University, Manhattan, KS-66506, USA, (e-mail: abujubbeh@ksu.edu; saimunikoti@ksu.edu; pahwa@ksu.edu; bala@ksu.edu)

A. Related work

Prior work on loss sensitivity analysis in distribution systems can be broadly grouped into two main categories: (1) analytical methods, and (2) classical load flow-based methods. As far as analytical methods are concerned, the most widely used method in the literature is based on computing nodal sensitivity factors [10], [11]. In this analytical method, the sensitivity of system losses is related to complex nodal changes through partial derivatives of line losses with respect to active or reactive power injection [12], [13]. The nodal sensitivity factor list helps reduce the search space when applying heuristic optimization algorithms for finding the best location or size of the DER [13]. For instance, in [14], [15] an analytical method is presented to find the optimal bus for installing DG in a power distribution system based on bus admittance matrix, generation information and load distribution of the system. Similarly, authors in [16], [17] propose a loss sensitivity-based method for placement of DERs in distribution systems. Here, loss sensitivity is used to examine the impact of DER injection on active power losses, which helps to determine optimal locations for DERs in the system [18]. Similar to nodal sensitivity factors, there are few analytical methods that focus on nodal allocation factors. The main idea of nodal allocation factors is to study the contribution of nodal complex power changes to system losses. Under this category, three popular types are typically used in literature: (1) incremental allocation method [19]; (2) Z-bus allocation [20] method, and (3) proportional sharing method [21]. In [19], nodal allocation factors are based on generator domains (the set of nodes that are supplied by each generator) and the set of commons (the set of nodes supplied by the same generator). The set of domains and commons are computed to determine the contribution of each generator to line flows, and thereby determine the contribution to line losses. Similarly, the z-bus allocation method is based on Z-bus matrix of the system (inverse of admittance matrix Y-bus). Authors in [20] use the Z-bus allocation method to determine incentive or penalties to nodal load increments considering system losses. However, such methods do not scale very-well with regard to computational complexity when the analysis is extended to large systems. When the size of the test system is small (e.g., 6 nodes [20]), it is difficult to generalize any method to real-world practical systems that are characterized by a large number of nodes. This is especially problematic when the method involves running multiple loops such as in (1) classical load flow analysis to capture DER variability [22], or (2) in the Z-bus allocation method to compute the set of domains and commons in the system. In addition, the incremental sharing method requires an algorithmic extension to be applicable for systems larger than 4 nodes [19]. Although nodal sensitivity factors help guide optimal DER planning strategies [23], results obtained from such methods are valid for a given scenario of power change. In this case, the nodal sensitivity factor list may differ across time considering dynamic load analysis, which unfortunately cannot be captured by traditional analytical loss sensitivity methods. Other approaches in the literature use polynomial chaos theory to compute voltage sensitivity in distribution systems [24]. Here, the approach involves finding basis polynomial functions to approximate the voltage change as a way to replace brute-force Monte Carlo simulations. However, the accuracy of this method depends greatly on the number of basis polynomials used to compute the voltage sensitivity. For example, for a 2 node distribution system with 4 loads, 15 polynomials are required to compute voltage sensitivity [24]. Additionally, the computational complexity of this method directly varies with the number of polynomials, resulting in an accuracy-complexity trade-off [24], [25]. Power loss sensitivity can also be determined using the classical load flow-based approach [26]. Here, the loss sensitivity is computed based on the voltage change due to complex power changes at different locations. In this regard, the change in voltage can be determined based on the Jacobian matrix of the system [27], i.e., partial derivatives of power flow equations with respect to nodal voltage magnitude and angles [22]. This can be used to determine the change in line current flows, which enables computing the changes in line power losses.

Most of the prior work on loss sensitivity considers computationally complex traditional methods of sensitivity analysis or traditional power flow equations. Such methods may not be adequate to address the needs of modern distribution systems for the following reasons. First, results obtained from such methods are scenario-specific and the inclusion of dynamic behavior of active consumers impacts their consistency. This hinders their applicability in real-time applications like finding the optimal location for EV charging or power loss monitoring [28]. Second, traditional sensitivity methods are computationally complex and require simulating a large number of scenarios to obtain the sensitivity of each scenario. It is important to note that the computational complexity of these methods increases with the increase in system size. Finally, in distribution systems, complex power changes at active consumer sites can be random due to variability in PV power outputs or dynamic load behaviors. This is unfortunately not considered in traditional analytical and load flow-based sensitivity methods. It should be noted that uncertainties of PV units (or DERs in general) can be captured by simulating a large number of scenarios, where the sensitivity can be computed. However, scenario-based analyses do not scale very well with increasing dimensions of variability. As we witness an increase in DER penetration, the number of scenarios needed for valid statistical inference grows exponentially. Alternatively, the proposed probabilistic approach in this paper is accurate, simple to implement, and scalable to large systems. This is because sampling random variables from well-established probability distributions is relatively (and consistently) faster. Therefore, this paper addresses these research gaps.

B. Contributions

This paper proposes a new probabilistic framework for loss sensitivity that helps to study the impact of changes in active consumer load patterns or DER injections on power loss in distribution systems. The major contributions of this work are listed below.

1) This work derives, for the first time, an analytical expression that approximates the changes in line current flows due to deterministic complex power variations at any node in the system (Theorem 1). The approximation error is shown to be upper bounded.
2) This work further develops analytical expressions to study the aggregate impact of multiple active consumers changing their complex power simultaneously on power losses in the system (Corollary 2).
3) The derived analytical expressions of line current and power loss changes are extended to account for variability associated with DER power injections at active consumer sites in the system resulting in a unique probabilistic sensitivity result. The Jensen-Shannon distance between the proposed and simulated loss probability distributions is in the order of 10^{-2}, which demonstrates the high accuracy of the proposed method.
4) The computational complexity of the proposed method is significantly lower than existing load flow-based methods, which enables a real-time loss monitoring feature that is necessary to guide optimal asset management in distribution systems.

The rest of the paper is organized as follows. Section II introduces the analytical approximation for the change in power losses in any line due to DER injections at any node in the system. Section III validates the proposed approximation and derives an upper bound on the approximation error. Section IV accounts for uncertainties in power injections and extends the proposed approach to a probabilistic framework to derive the probability distribution of change in line current flows and losses. Finally, section V concludes the paper with future research directions.

II. Analytical Framework for Loss Sensitivity

Consider a power distribution system with $\mathcal{N}$ nodes and $\mathcal{L}$ lines as illustrated in Fig. 1. The change in complex power at any node in the system causes changes in current flow in all lines, and thereby, causes changes in line power losses. Nodes where complex power varies are called *actor nodes* and lines where the change in current flow or power loss is monitored are called *monitored lines*. This section presents an analytical approximation for the change in line currents and

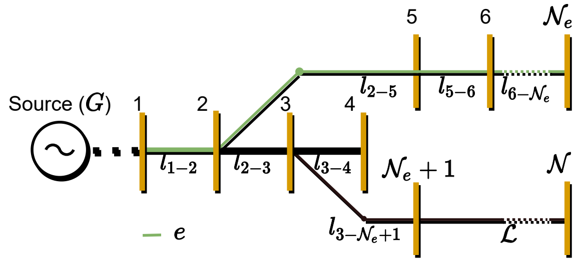

Figure 1: An illustration of a distribution system.

losses at any monitored line (M) due to change in complex power at actor nodes (A) in the system. When power at actor node A changes from S_A to $S_A + \Delta S_A$, the current at the monitored line changes from I_M to $I_M + \Delta I_{MA}$, where ΔI_{MA} is the change in current flow on the monitored line M due to complex power changes at actor node A. The reference node throughout this paper is assumed to operate at a unity voltage, i.e., $1\angle 0°$ p.u. Considering a single actor node, the change in current flow at the monitored line M can be approximated using Theorem 1.

Theorem 1. *For a single-phase distribution system, the change in current flow at a monitored line (M) due to change in complex power at an actor node (A) is approximated by,*

$$\Delta I_{MA} \approx \frac{\Delta S_A^* \Psi_{MA}}{V_A^*}, \tag{1}$$

where, ΔS_A^* is the complex conjugate of complex power change at actor node A, V_A^* is the complex conjugate of base voltage at the actor node A and Ψ_{MA} represents the influence indicator between node A and the origin node of line M. For nodes impacting the current flow on M, Ψ_{MA} can be set to 1 and 0 otherwise.

Proof. Consider a single-phase radial distribution system with $\mathcal{N}$ nodes and $\mathcal{L}$ lines with l_{m-n} representing the line connecting nodes m and n as shown in Fig. 1. Let e be the line connecting the set of nodes $\mathcal{N}_e$ with the source node G. The downstream current flowing through e can be written in terms of complex conjugate of power injections and nodal voltages as,

$$I_e = \sum_{k\in\mathcal{N}_e} I_k = \sum_{k\in\mathcal{N}_e} \frac{S_k^*}{V_k^*}. \tag{2}$$

When complex power changes at active consumer locations ($k \in \mathcal{N}_e$) from S_k to $S_k + \Delta S_k$, the voltage also changes from V_k to $V_k + \Delta V_k$. Therefore, the current flowing through e changes from I_e to $I_e^{'}$ and can be rewritten as,

$$I_e^{'} = \sum_{k\in\mathcal{N}_e} I_k^{'} = \sum_{k\in\mathcal{N}_e} \frac{S_k^* + \Delta S_k^*}{V_k^* + \Delta V_k^*}. \tag{3}$$

The change in line flow ($\Delta I_e = I_e^{'} - I_e$) at line e can be written as follows,

$$\Delta I_e = \sum_{k\in\mathcal{N}_e} \frac{S_k^* + \Delta S_k^*}{V_k^* + \Delta V_k^*} - \sum_{k\in\mathcal{N}_e} \frac{S_k^*}{V_k^*}$$
$$= \sum_{k\in\mathcal{N}_e} \frac{V_k^*(S_k^* + \Delta S_k^*) - S_k^*(V_k^* + \Delta V_k^*)}{V_k^*(V_k^* + \Delta V_k^*)}$$

Using assumption 2, we can rewrite ΔI_e as,

$$\Delta I_e \approx \sum_{k\in\mathcal{N}_e} \frac{\Delta S_k^*}{V_k^* + \Delta V_k^*} \tag{4}$$

Now assume that only one node (say node $A \in \mathcal{N}_e$) is changing its complex power. The corresponding change in line current can be written as,

$$\Delta I_e \approx \frac{\Delta S_A^*}{V_A^* + \Delta V_A^*} \tag{5}$$

The change in line flow can be written in terms of real and imaginary parts as follows,

$$\Delta I_e \approx \frac{\Delta P_A V_A^r(1 + \frac{\Delta V_A^r}{V_A^r}) + \Delta Q_A V_A^i(1 + \frac{\Delta V_A^i}{V_A^i})}{(V_A^r(1 + \frac{\Delta V_A^r}{V_A^r}))^2 + (V_A^i(1 + \frac{\Delta V_A^i}{V_A^i}))^2} + j\frac{\Delta P_A V_A^i(1 + \frac{\Delta V_A^i}{V_A^i}) - \Delta Q_A V_A^r(1 + \frac{\Delta V_A^r}{V_A^r})}{(V_A^r(1 + \frac{\Delta V_A^r}{V_A^r}))^2 + (V_A^i(1 + \frac{\Delta V_A^i}{V_A^i}))^2}, \tag{6}$$

where, V_A^r and V_A^i are the real and imaginary parts of actor node voltage, respectively. ΔP_A and ΔQ_A are the real and reactive power changes at actor node A. Now, using

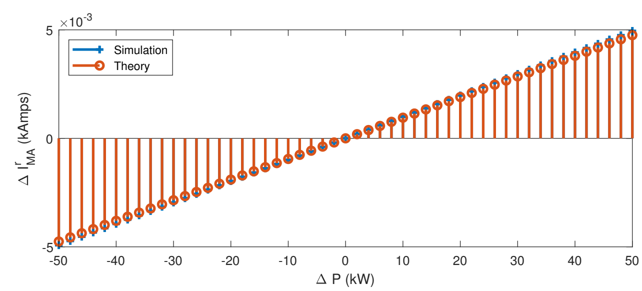

(a)

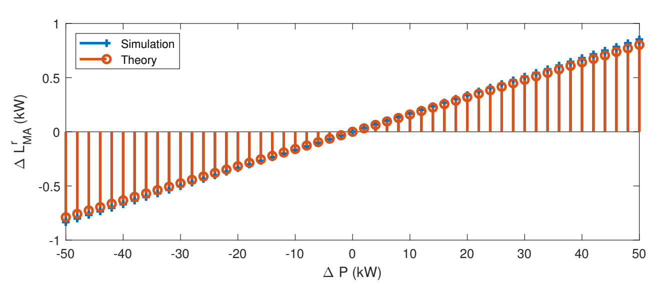

(b)

Figure 2: Sensitivity due to a single actor node: (a) change in line flow ΔI_{MA}. (b) change in active power losses ΔL_{MA}.

assumption 2, the change in real and imaginary parts of line current flow can be written as,

$$\Delta I_e \approx \frac{\Delta P_A V_A^r + \Delta Q_A V_A^i}{(V_A^r)^2 + (V_A^i)^2} + j\frac{\Delta P_A V_A^i - \Delta Q_A V_A^r}{(V_A^r)^2 + (V_A^i)^2} = \frac{\Delta S_A^*}{V_A^*} \tag{7}$$

For any monitored line $M \in e$, the change in current flow will only occur due to complex power changes at $A \in \mathcal{N}_e$ as shown in Fig. 1. Therefore, for any actor node $A \notin \mathcal{N}_e$, the influence factor Ψ_{MA} can be set to zero. That is,

$$\Delta I_{MA} \approx \frac{\Delta S_A^* \Psi_{MA}}{V_A^*}, \tag{8}$$

which completes the proof of Theorem 1. Below is a summary of the assumptions used throughout the proof of Theorem 1. □

Assumption 1. *The reference node operates at unity voltage, i.e.,* $1\angle 0°$ *p.u.*

Assumption 2. *In distribution systems, the change in nodal voltage relative to the actual nodal voltage is small.*

Assuming multiple actor nodes in the system change their complex power, the change in current flow through the monitored line M can be written as the sum effect of all individual changes as given in Corollary 1.

Corollary 1. *For a single-phase distribution system, the aggregate impact of complex power change at multiple actor nodes ($A \in \mathcal{A}$) on the change in current flow at a monitored line (M) is approximated by,*

$$\Delta I_M \approx \sum_{A\in\mathcal{A}} \frac{\Delta S_A^* \Psi_{MA}}{V_A^*}, \tag{9}$$

The current sensitivity due to multiple actor nodes is used to derive the loss sensitivity due to complex power change at active consumer sites.

Corollary 2. *For a single-phase distribution system, the aggregate impact of complex power change at multiple actor nodes ($A \in \mathcal{A}$) on the change in power loss at a monitored line (M) is approximated by,*

$$\Delta L_M \approx \Bigg[\sum_{A\in\mathcal{A}} \frac{\Delta S_A^* \Psi_{MA}}{V_A^*}^2 + 2\Re\Big(I_M^* \sum_{A\in\mathcal{A}} \frac{\Delta S_A^* \Psi_{MA}}{V_A^*}\Big)\Bigg] Z_M. \tag{10}$$

where, $Z_M = R_M + jX_M$ *is the impedance of the monitored line* M *and* I_M^* *is the complex conjugate of base current flow at line* M.

Proof. Consider again the system shown in Fig. 1. Power loss at a monitored line M can be written as [29],

$$L_M = |I_M|^2 Z_M \tag{11}$$
$$= L_{M,P} + jL_{M,Q} \tag{12}$$
$$= |I_M|^2 R_M + j|I_M|^2 X_M, \tag{13}$$

where $L_{M,P}$ and $L_{M,Q}$ are the active and reactive power losses at monitored line M, respectively. When the current flow at a monitored line M changes by ΔI_M, power loss at that line changes by ΔL_M and can be written as,

$$\Delta L_M = \Big[|I_M + \Delta I_M|^2 - |I_M|^2\Big] Z_M \tag{14}$$
$$= \Big[|\Delta I_M|^2 + 2\Re(I_M^* \Delta I_M)\Big] Z_M. \tag{15}$$

The change in current flow on that line (ΔI_M) can be computed using the analytical expression derived in Eq. (9). Therefore, the change in power loss at a monitored line M becomes,

$$\Delta L_M \approx \Bigg[\sum_{A\in\mathcal{A}} \frac{\Delta S_A^* \Psi_{MA}}{V_A^*}^2 + 2\Re\Big(I_M^* \sum_{A\in\mathcal{A}} \frac{\Delta S_A^* \Psi_{MA}}{V_A^*}\Big)\Bigg] Z_M. \tag{16}$$

□

A. Validation of analytical approximation

In this section, the proposed analytical approximation of the change in power losses is validated on the IEEE 69 node test system [30]. The base voltage of this test system is 12.66 kV and standard base loads are used for the analysis. Classical load flow method is used as a benchmark to evaluate the

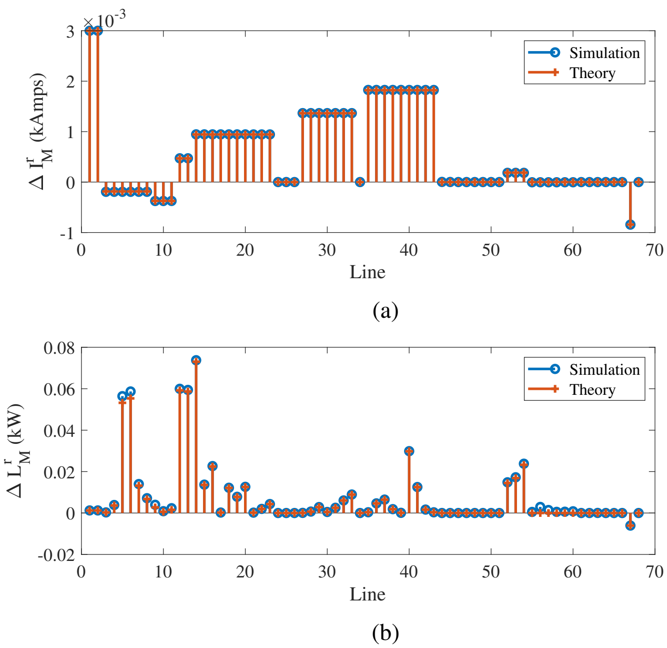

Figure 3: Sensitivity due to multiple actor nodes: (a) change in line flow ΔI_M. (b) change in active power losses ΔL_M.

Table I: Complex power change at multiple actor nodes.

Node	ΔS (kVA)	Base loading (kVA)
14	-5+j3	8+j5.5
24	10+j7	28+j20
34	15-j5	19.5+j14
44	20+j20	0
55	2+j2	24+j17.2
68	-9-j4	28+j20

accuracy of the proposed analytical approach. Two scenarios are created to show the accuracy of approximating the change in line current flow as well as losses. For the first scenario, node 15 is chosen randomly to change its complex power and the current and loss changes are monitored at line $5-6$, i.e., $\Delta I^r_{5,15}$ and $\Delta L^r_{5,15}$, where the superscript r represents the real part. Negative power change could represent increased DER injections (such as PV) or decreased load power. Similarly, positive power change can result from increased consumption or decrease in DER injection. Fig. 2 shows the changes in real line current and active losses where theory represents the proposed analytical expression and simulation is the result obtained via classical load flow-based method. It can be seen that the proposed analytical approach is accurate in approximating the change in line current and active power losses. The second scenario presents a case where power changes at randomly selected actor nodes. Table I reports the actor nodes and the respective values of complex power change as well as the base kVA loading. The change in real part of current flow and active losses for this scenario are illustrated in Fig. 3. As can be seen from the figure, the proposed method can approximate not only positive changes but also negative changes due to increased PV injection. This demonstrates the accuracy of the proposed method in approximating the change in line current flow and power loss. The proposed approach is generic and can also be applied in the presence of various binary equipment such as switches, tap changers, and switched capacitors. Such equipment are control action enablers that ensure optimal system operation, whereas the proposed sensitivity approach could be used as a precursor to such control actions. Specifically, the proposed analytical approach does not change due to the presence of switches, tap changers, or switching capacitors. However, thanks to the analytical nature of the proposed approach, it is a trivial task to account for such cases. Specifically, we only need to run the load flow once (or use recently proposed sparsity based distribution system state estimation approaches [31]) to get the base values of voltage, and thereafter the proposed analytical method can be applied to compute loss change at any monitored line of the system due to change in PV generation or load pattern. The complexity of the proposed method in terms of execution time is pretty much constant regardless of system size. This is one of the key strengths of the proposed approach. The following section derives an upper bound on the approximation error to ensure consistency of results obtained by the proposed analytical method.

III. Approximation Error Bound

This section further investigates the accuracy of the proposed approximation. First, the approximation error is computed and analytically upper-bounded. Thereafter, the bound on approximation error is verified using simulation scenarios tested on the IEEE 69 node test system.

Corollary 3. *For a single-phase distribution system, errors in approximating the changes in real and imaginary parts of line current flows (E^r_{MA} and E^i_{MA}, respectively) using (9) are upper bounded by,*

$$E^r \leq \sum_{A\in\mathcal{A}} \frac{\Delta P_A \Psi_{MA}}{V^r_A(1+\Phi_1)} + \frac{\Delta Q_A \Psi_{MA}}{V^i_A(1+\Phi_2)}, \tag{17}$$

$$E^i \leq \sum_{A\in\mathcal{A}} \frac{\Delta P_A \Psi_{MA}}{V^i_A(1+\Phi_2)} + \frac{\Delta Q_A \Psi_{MA}}{V^r_A(1+\Phi_1)}, \tag{18}$$

where, $\Phi_1 = \left(\frac{V^i_A}{V^r_A}\right)^2$ *and* $\Phi_2 = \Phi_1^{-1}$.

Proof. From Eq. (1), it can be seen that the voltage change compared to actual nodal voltage is small as in Eq. (6) and thus can be ignored, which yields the approximation in Eq. (7). The error resulting from the assumption that ($\frac{\Delta V^r_A}{V^r_A}$ and $\frac{\Delta V^i_A}{V^i_A} \approx 0$) is upper bounded by Corollary 3. We can compute the approximation error (for real part of change in current) as follows,

$$E^r = \Delta I^r_e - \Delta \hat{I}^r_e, \tag{19}$$

where ΔI^r_e is the actual change in real part of current flow and $\Delta \hat{I}^r_e$ is the approximated change in real part of current flow. Therefore,

$$\begin{aligned} E^r &= \left[\frac{\Delta P_A(V^r_A+\Delta V^r_A)}{(V^r_A+\Delta V^r_A)^2+(V^i_A+\Delta V^i_A)^2} - \frac{\Delta P_A V^r_A}{(V^r_A)^2+(V^i_A)^2}\right] \\ &+ \left[\frac{\Delta Q_A(V^i_A+\Delta V^i_A)}{(V^r_A+\Delta V^r_A)^2+(V^i_A+\Delta V^i_A)^2} - \frac{\Delta Q_A V^i_A}{(V^r_A)^2+(V^i_A)^2}\right] \\ &= E^r_1 + E^r_2 \end{aligned}$$

E^r_1 can be rewritten as,

$$E^r_1 = \frac{\Delta P_A(1+\frac{\Delta V^r_A}{V^r_A})}{V^r_A(1+\frac{\Delta V^r_A}{V^r_A})^2\left[1+\frac{(V^i_A)^2}{(V^r_A)^2}\frac{(1+\frac{\Delta V^i_A}{V^i_A})^2}{(1+\frac{\Delta V^r_A}{V^r_A})^2}\right]} - \frac{\Delta P_A}{V^r_A\left[1+\frac{(V^i_A)^2}{(V^r_A)^2}\right]}$$

Typically in distribution systems the change in nodal voltage compared to actual voltage is small, i.e., $\frac{\Delta V^r_A}{V^r_A} \approx 0$ and $\frac{\Delta V^i_A}{V^i_A} \approx 0$. Therefore, the previous equation can be rewritten as,

$$E^r_1 = \frac{\Delta P_A}{V^r_A(1+\Phi_1)}\left[\frac{1}{T^r} - 1\right]$$

where, $T^r = 1 + K^r$, $T^i = 1 + K^i$, $K^r = \frac{\Delta V^r_A}{V^r_A}$, $K^i = \frac{\Delta V^i_A}{V^i_A}$ and $\Phi_1 = \frac{(V^i_A)^2}{(V^r_A)^2}$. Considering the ratio of change in voltage to actual nodal voltage is small, the quantity $\frac{\Delta V_A^r}{V_A^r}$ will always be less than or equal to $1-\frac{\Delta V_A^r}{V_A^r}$, i.e.,

$$K^r \leq 1-K^r \Rightarrow \frac{K^r}{1-K^r} \leq 1 \Rightarrow \frac{1}{T^r}-1 \leq 1$$

$$\begin{aligned} \frac{\Delta P_A}{V_A^r(1+\Phi_1)}\left[\frac{1}{T^r}-1\right] &\leq \frac{\Delta P_A}{V_A^r(1+\Phi_1)} \\ \Rightarrow E_1^r &\leq \frac{\Delta P_A}{V_A^r(1+\Phi_1)} \\ \text{Similarly,} \quad E_2^r &\leq \frac{\Delta Q_A}{V_A^i(1+\Phi_2)}. \end{aligned} \tag{20}$$

Finally, by combining E_1^r and E_2^r, the error in approximating the real part of current change is upper bounded by,

$$E^r = E_1^r + E_2^r \leq \frac{\Delta P_A}{V_A^r(1+\Phi_1)} + \frac{\Delta Q_A}{V_A^i(1+\Phi_2)}. \tag{21}$$

Considering multiple actor nodes changing their complex power and repeating the same for imaginary part of current change yields,

$$E^r \leq \sum_{A\in\mathcal{A}} \frac{\Delta P_A \Psi_{MA}}{V_A^r(1+\Phi_1)} + \frac{\Delta Q_A \Psi_{MA}}{V_A^i(1+\Phi_2)}, \tag{22}$$

$$E^i \leq \sum_{A\in\mathcal{A}} \frac{\Delta P_A \Psi_{MA}}{V_A^i(1+\Phi_2)} + \frac{\Delta Q_A \Psi_{MA}}{V_A^r(1+\Phi_1)}, \tag{23}$$

which completes the proof of Corollary 3. □

The tightness of the upper bounds in Corollary 3 are validated via simulation on the IEEE 69 node test system. A simulation scenario is created where complex power varies at nodes 18 and 30 by $\Delta P = \Delta Q \in [-50, ..., 50]$ kW (and kVAr) and the change in current flow is monitored on line 5. The actual error is computed based on Eq. (19), i.e., the difference between numerical results using classical load flow and the proposed analytical approach. The error bound is computed based on the results provided by Corollary 3. Line 5 is randomly chosen to monitor line flow and compute the actual and approximation errors. However, the method is generic for any pair of actor nodes and monitored lines. Fig. 4 illustrates the actual error vs. the error bound for the aforementioned simulation scenario. The figure shows the errors in approximating real, imaginary and magnitude of current change. It can be seen from the figure that (17) and (18) present a tight upper bound for the actual error especially within the interval $[-20, ..., 20]$ kW (kVAr), which is consistent with real world power change scenarios. Therefore, the error bounds developed in Corollary 3 ensure the consistency and accuracy of the proposed analytical approach in approximating the change in line current. Next, this analytical framework is extended to account for variability associated with complex power injection (or withdrawal) at multiple active consumer sites in the system.

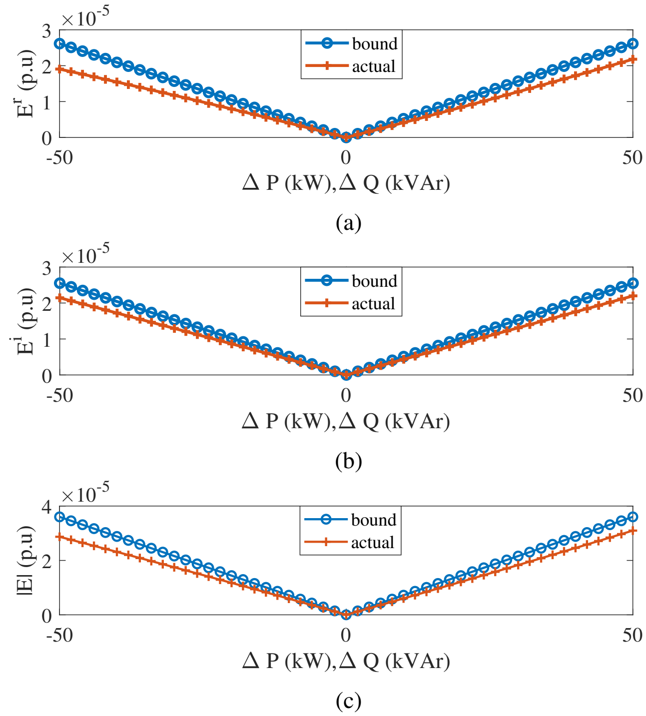

Figure 4: Approximation error bound using Corollary 3.

IV. Probabilistic loss sensitivity analysis

Complex power at active consumer sites could vary randomly due to the variability associated with DER injections (such as rooftop PV units and wind turbines) or due to dynamic load patterns. These stochastic processes inevitably impact system losses, which in turn leads to economic losses. Therefore, modern distribution system operators require an accurate, yet computationally efficient, loss monitoring tool that accounts for power uncertainties. This helps to guide optimal asset management strategies to keep losses minimal in a real-time fashion during electric vehicle planning or DER control. In this section, Corollaries 1 and 2 are used as the starting point to compute the probability distributions of change in current and power losses at a particular monitored line, respectively. Specifically, Eq. (8) can be rewritten as follows,

$$\Delta I_{MA} = \Delta I_{MA}^r + j\Delta I_{MA}^i,$$

where,

$$\begin{aligned} \Delta I_{MA}^r &\approx \frac{\Psi_{MA}(\Delta P_A \cos(\theta_A) - \Delta Q_A \sin(\theta_A))}{|V_A|} \\ \Delta I_{MA}^i &\approx \frac{\Psi_{MA}(-\Delta P_A \sin(\theta_A) - \Delta Q_A \cos(\theta_A))}{|V_A|}. \end{aligned} \tag{24}$$

Here, θ_A is the voltage angle of actor node A. Since multiple actor nodes impact the current flow at line M, using Corollaries 1 and 2, we conclude that

$$\Delta I_M = \sum_{A\in\mathcal{A}} \Delta I_{MA}^r + j \sum_{A\in\mathcal{A}} \Delta I_{MA}^i, \tag{25}$$

$$\begin{aligned}\Delta L_M = &\left[\sum_{A\in\mathcal{A}} \Delta I_{MA}^{\ 2} + 2\Re\Big(I_M^* \sum_{A\in\mathcal{A}} \Delta I_{MA}\Big)\right] R_M \\ &+ j\left[\sum_{A\in\mathcal{A}} \Delta I_{MA}^{\ 2} + 2\Re\Big(I_M^* \sum_{A\in\mathcal{A}} \Delta I_{MA}\Big)\right] X_M.\end{aligned} \tag{26}$$

DER injection or dynamic load patterns can be modeled as a probability distribution to account for the variability. In particular, complex power changes (withdrawal or injection) at active consumer sites can be modeled as a random vector $\boldsymbol{\Delta s} = [\Delta P_1, ..., \Delta P_N, \Delta Q_1, ..., \Delta Q_N]^T$ with mean $\boldsymbol{\mu} = \mathbf{0}$ and a covariance structure captured by the covariance matrix $\boldsymbol{\Sigma_{\Delta s}}$. The following subsections highlight the steps followed to derive the probability distribution of the squared magnitude of the change in current flow that is used in Eq. (26) to compute line losses.

A. Construct $\boldsymbol{\Sigma_{\Delta s}}$ and compute $\boldsymbol{k_r}$ and $\boldsymbol{k_i}$

$\boldsymbol{\Sigma_{\Delta s}}$ contains information about the variance of complex power change at active consumer locations that represents, for instance, the size of PV unit or the load pattern, etc. Off-diagonal elements of the covariance matrix capture the spatial correlation of complex power changes at different actor nodes. The spatial correlation is a byproduct of the geographical proximity of renewable energy sources. The covariance matrix depends on the size of the system and the number of active consumers changing their complex power as shown in Eq. (28) below. p_i and q_i are the active and reactive power injection or consumption at the i^{th} active consumer site, respectively, whereas $n \triangleq \mathcal{N}$ is the system size. The exact $\boldsymbol{\Sigma_{\Delta s}}$ of a particular system can be estimated based on historical data as discussed in [32], and is out of the scope of this work. If a node does not have DER units, the variance of complex power of that node can be set to zero and the standard kVA loading of that node will be used for the analysis. Additionally, the constant terms in (24) are arranged in $\boldsymbol{k}_r$ and $\boldsymbol{k}_i$ vectors. These vectors are functions of the magnitude of nodal base voltages and the nodal-line sensitivity relationships based system topology (defined by Ψ_{MA}). For each system, these vectors are fixed and can be readily computed using Eq. (27). It is important to note that the proposed analytical methodology to compute loss change is generic and is valid for any type of distribution system. However, steps to compute the intermediate values of the final loss expression could vary with the system topology. For instance, the procedure to determine Ψ_{MN} values of the weight vectors in (27) could vary with the system topology. The theoretical derivation of exact expressions for other system topology will be pursued as part of future work.

$$\boldsymbol{k}_r = \begin{bmatrix} \frac{\Psi_{M1}\cos\theta_1}{|V_1|} \\ \frac{\Psi_{M2}\cos\theta_1}{|V_2|} \\ \vdots \\ \frac{\Psi_{M\mathcal{N}}\cos\theta_{\mathcal{N}}}{|V_{\mathcal{N}}|} \\ -\frac{\Psi_{M1}\sin\theta_1}{|V_1|} \\ -\frac{\Psi_{M2}\sin\theta_1}{|V_2|} \\ \vdots \\ -\frac{\Psi_{M\mathcal{N}}\sin\theta_{\mathcal{N}}}{|V_{\mathcal{N}}|} \end{bmatrix}_{2\mathcal{N}\times 1} \qquad \boldsymbol{k}_i = \begin{bmatrix} -\frac{\Psi_{M1}\sin\theta_1}{|V_1|} \\ -\frac{\Psi_{M2}\sin\theta_1}{|V_2|} \\ \vdots \\ -\frac{\Psi_{M\mathcal{N}}\sin\theta_{\mathcal{N}}}{|V_{\mathcal{N}}|} \\ -\frac{\Psi_{M1}\cos\theta_1}{|V_1|} \\ -\frac{\Psi_{M2}\cos\theta_1}{|V_2|} \\ \vdots \\ -\frac{\Psi_{M\mathcal{N}}\cos\theta_{\mathcal{N}}}{|V_{\mathcal{N}}|} \end{bmatrix}_{2\mathcal{N}\times 1} \tag{27}$$

Here, $\boldsymbol{\theta} = [\theta_1, ..., \theta_{\mathcal{N}}]^T$ represents the base voltage angles.

B. Compute the distribution of ΔI_M^r and ΔI_M^i

It can be seen from Eq. (9) that the change in line current flows at a monitored line can be expressed as the aggregate changes in current flows caused by every actor node in the system. Now, consider random changes in complex power at actor nodes as given by the covariance matrix in Eq. (28). Using the Lindeberg-Feller central limit theorem, each of the probability distributions of ΔI_M^r and ΔI_M^i can be shown to converge to a Gaussian distribution as,

$$\Delta I_M^r = \sum_{A\in\mathcal{A}} \Delta I_{MA}^r \approx \boldsymbol{k}_r^T \boldsymbol{\Delta s} \xrightarrow{D} \mathcal{N}(0, \boldsymbol{k}_r^T \boldsymbol{\Sigma_{\Delta s}} \boldsymbol{k}_r), \tag{29}$$

$$\Delta I_M^i = \sum_{A\in\mathcal{A}} \Delta I_{MA}^i \approx \boldsymbol{k}_i^T \boldsymbol{\Delta s} \xrightarrow{D} \mathcal{N}(0, \boldsymbol{k}_i^T \boldsymbol{\Sigma_{\Delta s}} \boldsymbol{k}_i). \tag{30}$$

Here, $\mathcal{A}$ is the set of actor nodes resulting in the change of current flow at line M. The terms $\boldsymbol{k}_r^T \boldsymbol{\Sigma_{\Delta s}} \boldsymbol{k}_r \triangleq \sigma_r^2$ and $\boldsymbol{k}_i^T \boldsymbol{\Sigma_{\Delta s}} \boldsymbol{k}_i \triangleq \sigma_i^2$ represent the variances of ΔI_M^r and ΔI_M^i, respectively.

C. Compute the distribution of $|\Delta I_M|^2$

The squared magnitude of current change at a monitored line M can be written as,

$$|\Delta I_M|^2 = (\Delta I_M^r)^2 + (\Delta I_M^i)^2. \tag{31}$$

Since the probability distributions of ΔI_M^r and ΔI_M^r converge to Gaussian distributions, the square of a Gaussian distribution, i.e., $(\Delta I_M^r)^2$ and $(\Delta I_M^i)^2$, follows a Gamma distribution with 0.5 as the shape parameter and scale parameter twice the variance of the Gaussian distribution [33]. That is,

$$(\Delta I_M^r)^2 \sim \Gamma(0.5, 2\sigma_r^2) \tag{32}$$

$$(\Delta I_M^i)^2 \sim \Gamma(0.5, 2\sigma_i^2) \tag{33}$$

Typically, in distribution systems the change in real and imaginary parts of current flow are correlated. In the proposed analytical method, this correlation is captured by Eq. (28) and (27). That is, the Gamma distributions in Eq. (32) and (33) are correlated by $K \triangleq \boldsymbol{k}_r^T \boldsymbol{\Sigma_{\Delta s}} \boldsymbol{k}_i$. The sum of correlated Gamma distributions $\Gamma(0.5, 2\sigma_r^2)$ and $\Gamma(0.5, 2\sigma_i^2)$ also follows a Gamma distribution [34],

$$|\Delta I_M|^2 = (\Delta I_M^r)^2 + (\Delta I_M^i)^2 \sim \Gamma(k, \theta), \tag{34}$$

with scale and shape parameters $k = \frac{(\sigma_r^2+\sigma_i^2)}{\theta}$ and $\theta = \frac{2(\sigma_r^4+\sigma_i^4+2K^2)}{\sigma_r^2+\sigma_i^2}$, respectively.

$$
\mathbf{\Sigma_{\Delta S}} = \begin{bmatrix} \sigma_{p_1}^2 & \dots & cov(p_n,p_1) & cov(q_1,p_1) & \dots & cov(q_n,p_1) \\ \vdots & \ddots & \vdots & \vdots & \ddots & \vdots \\ cov(p_1,p_n) & \dots & \sigma_{p_n}^2 & cov(q_1,p_n) & \dots & cov(q_n,q_n) \\ cov(p_1,q_1) & \dots & cov(p_n,q_1) & \sigma_{q_1}^2 & \dots & cov(q_n,p_1) \\ \vdots & \ddots & \vdots & \vdots & \ddots & \vdots \\ cov(p_1,q_n) & \dots & cov(p_n,q_n) & cov(q_1,q_n) & \dots & \sigma_{q_n}^2 \end{bmatrix}_{2\mathcal{N}\times 2\mathcal{N}} \tag{28}
$$

D. Compute the distribution of ΔL_M^r and ΔL_M^i

This subsection derives the probability distribution of ΔL_M^r and ΔL_M^i based on the approximation in Corollary 2. The change in power loss at a monitored line M can be written in terms of real and imaginary parts as,

$$
\begin{aligned}
\Delta L_M &= \Delta L_M^r + j\Delta L_M^i \\
&= \Big[|\Delta I_M|^2 + 2\Re(I_M^* \Delta I_M)\Big] R_M \\
&\quad + j\Big[|\Delta I_M|^2 + 2\Re(I_M^* \Delta I_M)\Big] X_M
\end{aligned}
$$

From (34), $|\Delta I_M|^2 \sim \Gamma(k,\theta)$. Therefore,

$$
\Delta L_M^r = \Big[\Gamma(k,\theta) + 2\Re(I_M^* \Delta I_M)\Big] R_M \text{ and,}
$$

$$
\Delta L_M^i = \Big[\Gamma(k,\theta) + 2\Re(I_M^* \Delta I_M)\Big] X_M.
$$

If $X \sim \Gamma(k,\theta)$, then, $\forall a > 0, \quad aX \sim \Gamma(k, a\theta)$. Thus,

$$
\Delta L_M^r = \Gamma(k, R_M\theta) + 2R_M\Re(I_M^* \Delta I_M), \tag{35}
$$

$$
\Delta L_M^i = \Gamma(k, X_M\theta) + 2X_M\Re(I_M^* \Delta I_M). \tag{36}
$$

Fig. 5 shows a brief flowchart explaining the steps behind computing the probability distribution of change in active power losses using the proposed analytical approach.

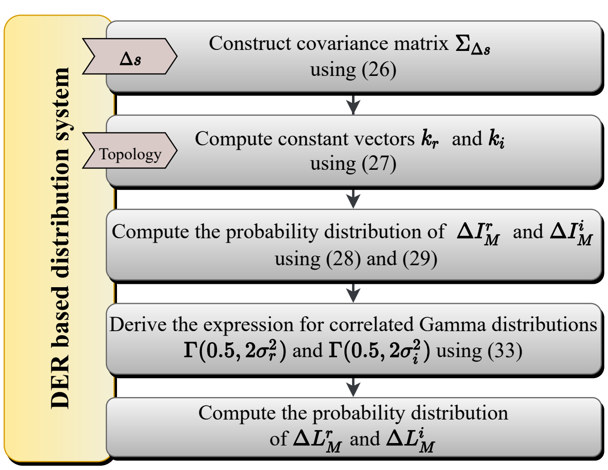

Figure 5: A flowchart of the proposed analytical PLSA approach.

E. Validation via simulation

This section validates the theoretical expressions derived earlier to compute the probability distributions of current and loss changes. For simplicity of demonstration, only the real parts of both current and loss sensitivity analysis is shown. However, the proposed analytical approach is generic and can be applied to the imaginary parts as well. The proposed PLSA method is verified on the same IEEE 69 node test system. A scenario is created where complex power varies at a randomly selected set of actor nodes $A \in [5, 7, ..., 25]$ and the change in current and power losses are monitored on line $10-11$. It is assumed that actor nodes are integrated with PV units. To account for the variability in PV power outputs, complex power change ($\mathbf{\Delta s}$) among actor nodes is assumed to be random following a zero-mean Gaussian distribution with the covariance structure shown in Eq. (28). Although we assume a Gaussian distribution for power changes, the proposed method is generic to any choice of probability distribution. Additionally, PV power injection among actor nodes is correlated due to geographical proximity. Therefore, $\mathbf{\Sigma_{\Delta s}}$ captures those relationships by the off-diagonal covariance terms. For this particular case study, $\mathbf{\Sigma_{\Delta s}}$ is defined as follows. Active power variance on the diagonal is set to be 15 kW for nodes integrated with PV units. The reactive power variance for those nodes is set to 10 kVAr. For off-diagonal elements relating the change in active power among actor nodes, i.e., $cov(\Delta P_i, \Delta P_k) = 0.7$ where $i, j \in \boldsymbol{\mathcal{A}}$ and $i \neq j$. Furthermore, the covariance of change in reactive power $cov(\Delta Q_i, \Delta Q_k)$ is set to 0.6. Finally, the covariance between active and reactive power change $cov(\Delta P_i, \Delta Q_k)$ is set to 0.3. Variance and covariance of PV units in this scenario are kept the same for all actor nodes. However, the proposed approach is generic to accommodate various types of $\mathbf{\Sigma_{\Delta s}}$ structures.
The proposed analytical approach is compared to the benchmark results obtain by classical load flow-based sensitivity method. For the proposed analytical approach, firstly, the $\boldsymbol{k}_r$ and $\boldsymbol{k}_i$ are computed using Eq. (27), respectively. Then, the variance and covariance terms of change in real and imaginary parts of current are computed as,

$$
\begin{aligned}
\mathbf{\Sigma}_{\Delta I_M} &= \begin{bmatrix} \boldsymbol{k}_r^T \mathbf{\Sigma_{\Delta s}} \boldsymbol{k}_r & \boldsymbol{k}_i^T \mathbf{\Sigma_{\Delta s}} \boldsymbol{k}_r \\ \boldsymbol{k}_i^T \mathbf{\Sigma_{\Delta s}} \boldsymbol{k}_r & \boldsymbol{k}_i^T \mathbf{\Sigma_{\Delta s}} \boldsymbol{k}_i \end{bmatrix} \\
&= \begin{bmatrix} 0.8351 & -0.0354 \\ -0.0354 & 0.0787 \end{bmatrix} \times 10^{-3}.
\end{aligned} \tag{37}
$$

Thereafter, the distribution of change in real part of current is computed by sampling random variables using Eq. (29). For

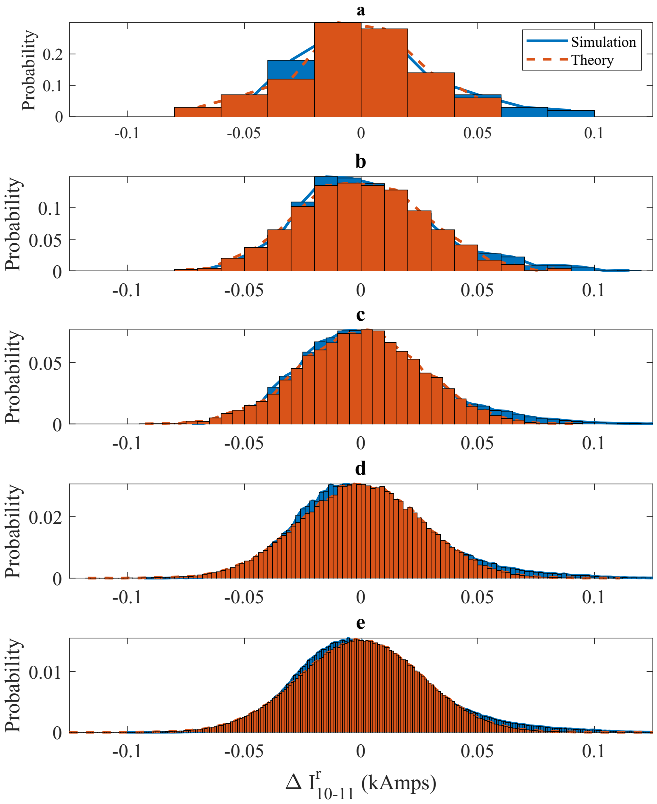

Figure 6: Probability distribution of change in real part of current flow ΔI_M^r for cases a, b, c, d and e.

the benchmark results, load flow scenarios are created using the covariance matrix defined in (28). To illustrate the efficacy of the proposed approach, five different cases (namely case $a, b, c, d,$ and e) are created by varying the number of load flow scenarios (as well as the number of random variables sampled with the proposed analytical approach). Specifically, we choose 100 simulations vs. 100 random variables, $1k$ simulations vs. $1k$ random variables, $10k$ simulations vs. $10k$ random variables, $100k$ simulations vs. $100k$ random variables, and $1m$ simulations vs. $1m$ random variables, for cases, $a, b, c, d,$ and e, respectively. Fig. 6 shows the distribution of real part of current change on line 10-11 for all cases using the proposed analytical approach (red) compared to the simulation based method (blue). It can be inferred from the figure that the probability distributions shown in cases $a, b, c,$ and d are less accurate than the distributions in case e. This is because the accuracy of the probability distribution improves with the increased number of scenarios (or number of random variables in the case of the proposed probabilistic approach). In order to make these comparisons objective, we use the Jensen-Shannon distance (JSD), an information-theoretic similarity measure, to validate the accuracy of the proposed probabilistic approximation (compared to simulation-based classical load flow method) of both distributions of change in current flow as well as active power losses. The similarity (or JSD) between simulations based and theoretical distributions can be

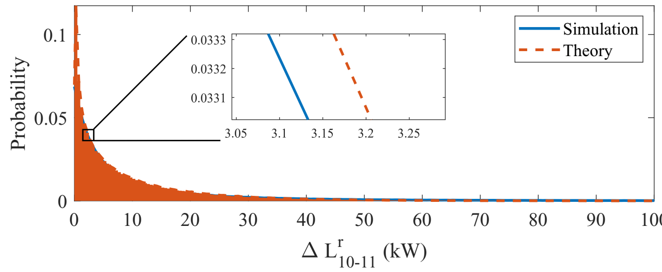

Figure 7: Probability distribution of change in active power losses ΔL_M^r.

computed as [35],

$$\text{JSD}(P||Q) = \frac{1}{2} D_{KL}(P||M) + \frac{1}{2} D_{KL}(Q||M), \tag{38}$$

where, $M = \frac{1}{2}(P+Q)$ and D_{KL} is the Kullback-Leibler (KL) divergence metric as a measure of the information lost when Q is used to approximate P evaluated at the support $x \in \mathcal{X}$ and can be written as,

$$D_{KL}(P||Q) = \sum_{x \in \mathcal{X}} P(x) \log \left(\frac{P(x)}{Q(x)} \right) \tag{39}$$

The JSD distance is used for validation instead of the KL divergence because the JSD is always symmetric, well defined, and bounded [36]. JSD can vary between 0 (meaning the two distributions are identical) and 1 (meaning the distributions are completely different). The JSD between actual simulation-based and theoretical distributions of change in current flow is in the order of 10^{-2}, which implies that the probabilistic approximation is accurate when compared to existing simulation-based method.

Subsequently, the shape and scale parameters of the Gamma distribution in Eq. (34) are computed as $k = 0.5913$ and $\theta = 0.0015$ to obtain the probability distribution of the change in active power loss on line $10-11$ using Eq. (35). The distribution of change in active power losses is computed for case e and illustrated in Fig. 7. The JSD between actual simulation-based and theoretical distribution of change in active power loss is found to be in the order of 10^{-2}. These results imply that it is possible to accurately evaluate the probability of line current flow or active power losses exceeding a certain threshold (γ). For instance, Table II shows the probability of real part of current change exceeding $\gamma_c = 0.002$ kAmps and active losses exceeding $\gamma_l = 0.5$ kW using classical method and the proposed analytical approach.

Finally, the computational complexity of the proposed method is compared via the execution time taken to compute the probability distributions of change in current and power loss for a given monitored line M, in this case, line $10-11$.

Table II: Probability of exceeding the threshold γ.

Probability	Simulation	Theory
$\mathbb{P}(\lvert\Delta I_M^r\rvert > \gamma_c)$	0.8630	0.8561
$\mathbb{P}(\lvert\Delta L_M^r\rvert > \gamma_l)$	0.9404	0.9396

Table III: Execution time (s).

Case	Simulation	Theory
case a	0.2897	0.0472
case b	2.1852	0.0482
case c	19.1739	0.0694
case d	190.4614	0.0934
case e	1871.84421	0.2373

The analysis is implemented with intel i-9 processor for all cases illustrated in Fig. 6 and the corresponding execution time taken by both approaches is reported in Table III. The proposed analytical approach outperforms the classical simulation based method regardless of the number of simulations (or random variables in the case of the proposed approach) used to obtain the probability density curves. This is because sampling random variables from well-established probability distributions is faster compared the classical scenario-based analysis, which require simulating large number of scenarios to achieve the required accuracy. This implies that the proposed analytical framework accurately approximates the distribution of change in current flow and in line losses with significantly lower computational effort. It is important to note that the computational efficiency of the proposed approach is consistent regardless of system size or choice of monitored lines. Therefore, with the proposed approach, it is possible to significantly simplify the process of loss monitoring in modern distribution systems, which enables various downstream applications such as EV and DER planning.

V. Conclusion

This paper proposes a new probabilistic loss sensitivity analysis framework that builds off an analytical approximation of the change in power losses at a given line due to complex power changes at other nodes in the system. First, an analytical expression is derived to compute the change in line losses for deterministic power changes at one actor node. Then, the effect of random power changes at multiple active consumer sites is examined using the proposed approach. It is shown that the probability distribution of change in line power losses is well approximated by a Gamma distribution. The proposed analytical expressions are validated via simulations on the IEEE 69 node test system. Simulation results show that approximating the change in power loss at any line in the system is highly accurate with a JSD in the order of 10^{-2}. In addition, the proposed approach is computationally efficient when compared to traditional load flow-based sensitivity methods. The computational advantage of the proposed approach makes it a suitable tool for real-time optimal resource management to minimize losses. Future work includes extending the probabilistic loss sensitivity analysis for 3-phase unbalanced distribution systems with wide variety of network topologies.

VI. ACKNOWLEDGMENT

This paper is based upon work supported by the National Science Foundation under Grant No. # 1855216. Any opinions, findings, and conclusions or recommendations expressed in this paper are those of the authors and do not necessarily reflect the views of the National Science Foundation.

References

[1] A. Ehsan and Q. Yang, "Optimal integration and planning of renewable distributed generation in the power distribution networks: A review of analytical techniques," *Applied Energy*, vol. 210, pp. 44–59, 2018.

[2] K. E. Adetunji, I. W. Hofsajer, A. M. Abu-Mahfouz, and L. Cheng, "Category-based multiobjective approach for optimal integration of distributed generation and energy storage systems in distribution networks," *IEEE Access*, vol. 9, pp. 28 237–28 250, 2021.

[3] C. Zhang and Y. Xu, "Hierarchically-coordinated voltage/var control of distribution networks using pv inverters," *IEEE Transactions on Smart Grid*, vol. 11, no. 4, pp. 2942–2953, 2020.

[4] H. Mortazavi, H. Mehrjerdi, M. Saad, S. Lefebvre, D. Asber, and L. Lenoir, "A monitoring technique for reversed power flow detection with high pv penetration level," *IEEE Transactions on Smart Grid*, vol. 6, no. 5, pp. 2221–2232, 2015.

[5] P. Rajesh and F. H. Shajin, "Optimal allocation of ev charging spots and capacitors in distribution network improving voltage and power loss by quantum-behaved and gaussian mutational dragonfly algorithm (qgda)," *Electric Power Systems Research*, vol. 194, p. 107049, 2021.

[6] W. Sheng, K.-Y. Liu, Y. Liu, X. Meng, and Y. Li, "Optimal placement and sizing of distributed generation via an improved nondominated sorting genetic algorithm ii," *IEEE Transactions on Power Delivery*, vol. 30, no. 2, pp. 569–578, 2014.

[7] P. Díaz, M. Pérez-Cisneros, E. Cuevas, O. Camarena, F. A. F. Martinez, and A. González, "A swarm approach for improving voltage profiles and reduce power loss on electrical distribution networks," *IEEE Access*, vol. 6, pp. 49 498–49 512, 2018.

[8] Q. Peng, Y. Tang, and S. H. Low, "Feeder reconfiguration in distribution networks based on convex relaxation of opf," *IEEE Transactions on Power Systems*, vol. 30, no. 4, pp. 1793–1804, 2014.

[9] M. H. Amini, M. P. Moghaddam, and O. Karabasoglu, "Simultaneous allocation of electric vehicles' parking lots and distributed renewable resources in smart power distribution networks," *Sustainable cities and society*, vol. 28, pp. 332–342, 2017.

[10] J. Guerrero, A. C. Chapman, and G. Verbic, "Decentralized p2p energy trading under network constraints in a low-voltage network," *IEEE Transactions on Smart Grid*, vol. 10, no. 5, pp. 5163–5173, 2018.

[11] B. Singh and D. K. Mishra, "A survey on enhancement of power system performances by optimally placed dg in distribution networks," *Energy Reports*, vol. 4, pp. 129–158, 2018.

[12] R. S. Rao, K. Ravindra, K. Satish, and S. Narasimham, "Power loss minimization in distribution system using network reconfiguration in the presence of distributed generation," *IEEE transactions on power systems*, vol. 28, no. 1, pp. 317–325, 2012.

[13] Y. Li, B. Feng, G. Li, J. Qi, D. Zhao, and Y. Mu, "Optimal distributed generation planning in active distribution networks considering integration of energy storage," *Applied energy*, vol. 210, pp. 1073–1081, 2018.

[14] C. Wang and M. H. Nehrir, "Analytical approaches for optimal placement of distributed generation sources in power systems," *IEEE Transactions on Power systems*, vol. 19, no. 4, pp. 2068–2076, 2004.

[15] C. Wang and M. Nehrir, "Analytical approaches for optimal placement of distributed generation sources in power systems," in *IEEE Power Engineering Society General Meeting, 2005*. IEEE, 2005, pp. 2393–Vol.

[16] H. Hedayati, S. A. Nabaviniaki, and A. Akbarimajd, "A method for placement of dg units in distribution networks," *IEEE transactions on power delivery*, vol. 23, no. 3, pp. 1620–1628, 2008.

[17] M. Kashem, A. D. Le, M. Negnevitsky, and G. Ledwich, "Distributed generation for minimization of power losses in distribution systems," in *2006 IEEE Power Engineering Society General Meeting*. IEEE, 2006, pp. 8–pp.

[18] V. M. Quezada, J. R. Abbad, and T. G. S. Roman, "Assessment of energy distribution losses for increasing penetration of distributed generation," *IEEE Transactions on power systems*, vol. 21, no. 2, pp. 533–540, 2006.

[19] D. Kirschen, R. Allan, and G. Strbac, "Contributions of individual generators to loads and flows," *IEEE Transactions on power systems*, vol. 12, no. 1, pp. 52–60, 1997.

[20] A. J. Conejo, F. D. Galiana, and I. Kockar, "Z-bus loss allocation," *IEEE Transactions on Power Systems*, vol. 16, no. 1, pp. 105–110, 2001.

[21] J. Bialek, “Tracing the flow of electricity,” *IEE Proceedings-Generation, Transmission and Distribution*, vol. 143, no. 4, pp. 313–320, 1996.
[22] F. Tamp and P. Ciufo, “A sensitivity analysis toolkit for the simplification of mv distribution network voltage management,” *IEEE Transactions on Smart Grid*, vol. 5, no. 2, pp. 559–568, 2014.
[23] F. Rotaru, G. Chicco, G. Grigoras, and G. Cartina, “Two-stage distributed generation optimal sizing with clustering-based node selection,” *International journal of electrical power & energy systems*, vol. 40, no. 1, pp. 120–129, 2012.
[24] A. Koirala, T. Van Acker, D. Van Hertem, J. Camargo, and R. D’hulst, “General polynomial chaos vs crude monte carlo for probabilistic evaluation of distribution systems,” in *2020 International Conference on Probabilistic Methods Applied to Power Systems (PMAPS)*. IEEE, 2020, pp. 1–6.
[25] J. Laowanitwattana and S. Uatrongjit, “Probabilistic power flow analysis based on arbitrary polynomial chaos expansion for networks with uncertain renewable sources,” *IEEJ transactions on Electrical and Electronic Engineering*, vol. 13, no. 12, pp. 1754–1759, 2018.
[26] J. Lu, L. L. Zhang, D. Y. Shi, T. Li, J. C. Tang, and D. Cui, “On-line data splicing power flow analysis method based on sensitivity,” *Energy Reports*, vol. 7, pp. 326–333, 2021.
[27] J. Dancker, C. Klabunde, and M. Wolter, “Sensitivity factors in electricity-heating integrated energy systems,” *Energy*, vol. 229, p. 120600, 2021.
[28] W. Wu and B. Lin, “Benefits of electric vehicles integrating into power grid,” *Energy*, vol. 224, p. 120108, 2021.
[29] L. Ramesh, S. Chowdhury, S. Chowdhury, A. Natarajan, and C. Gaunt, “Minimization of power loss in distribution networks by different techniques,” *International Journal of Electrical Power and Energy Systems Engineering*, vol. 2, no. 1, pp. 1–6, 2009.
[30] I. Power and E. Society, “Ieee pes amps dsas test feeder working group,” https://site.ieee.org/pes-testfeeders/resources/.
[31] S. Dahale, H. S. Karimi, K. Lai, and B. Natarajan, “Sparsity based approaches for distribution grid state estimation-a comparative study,” *IEEE Access*, vol. 8, pp. 198 317–198 327, 2020.
[32] C. Muscas, M. Pau, P. A. Pegoraro, and S. Sulis, “Effects of measurements and pseudomeasurements correlation in distribution system state estimation,” *IEEE Transactions on Instrumentation and Measurement*, vol. 63, no. 12, pp. 2813–2823, 2014.
[33] H. O. Lancaster and E. Seneta, “Chi-square distribution,” *Encyclopedia of biostatistics*, vol. 2, 2005.
[34] L.-L. Chuang and Y.-S. Shih, “Approximated distributions of the weighted sum of correlated chi-squared random variables,” *Journal of Statistical Planning and Inference*, vol. 142, no. 2, pp. 457–472, 2012.
[35] S.-C. Tsai, W.-G. Tzeng, and H.-L. Wu, “On the jensen-shannon divergence and variational distance,” *IEEE transactions on information theory*, vol. 51, no. 9, pp. 3333–3336, 2005.
[36] A. Majtey, P. Lamberti, and D. Prato, “Jensen-shannon divergence as a measure of distinguishability between mixed quantum states,” *Physical Review A*, vol. 72, no. 5, p. 052310, 2005.

Mohammad Abujubbeh (S’20) received his B.Sc. in Electrical & Electronic Engineering from Eastern Mediterranean University, Famagusta, Cyprus in 2016. He was a M.Sc. student of Sustainable Environment and Energy Systems at Middle East Technical University, from 2017 to 2019. He is presently with Kansas State University pursuing his Ph.D. in Electrical and Computer Engineering. His research interests include cyber-physical systems, renewable energy integration, probabilistic loss sensitivity analysis and IoT-enabled smart grids.

Sai Munikoti (S’19) received the B.Tech. degree in electrical engineering from the Birsa Institute of Technology Sindri, India, in 2015, and the M.Tech. degree in electrical engineering from Indian Institute of Technology Gandhinagar, India, in 2018. He is currently pursuing Ph.D. with the department of Electrical and Computer engineering at Kansas State University, Manhattan, KS, USA. His research interests spans areas of power distribution system, graph theory, machine learning, and resilience analysis.

Anil Pahwa (F’03) received the B.E. (Hons.) degree in electrical engineering from the Birla Institute of Technology and Science, Pilani, India, in 1975, the M.S. degree in electrical engineering from the University of Maine, Orono, ME, USA, in 1979, and the Ph.D. degree in electrical engineering from the Texas A&M University, College Station, TX, USA, in 1983. Since 1983, he has been with Kansas State University, Manhattan, KS, USA, where he is currently a University Distinguished Professor and holds the LoganFetterhoof Chair in the Electrical and Computer Engineering Department. The National Academy selected him as a Jefferson Science Fellow in 2014 to serve as a Senior Science Advisor in the U.S. State Department for one year. He was with the East Asian and Pacific Affairs Bureau on international policies to facilitate higher deployment of renewable energy. His research interests include distribution automation, distribution planning, renewable energy integration into power systems, and intelligent computational methods for distribution system applications.

Balasubramaniam Natarajan (SM’08) received the B.E. degree (Hons.) in electrical and electronics engineering from the Birla Institute of Technology and Science at Pilani, Pilani, India, in 1997, the Ph.D. degree in electrical engineering from Colorado State University, Fort Collins, CO, USA, in 2002, and the Ph.D. degree in statistics from Kansas State University, Manhattan, KS, USA, in 2018. He is currently a Clair N. Palmer and Sara M. Palmer Endowed Professor and the Director of the Wireless Communication and Information Processing Research Group, Kansas State University. He has worked on and published extensively on modeling, analysis and networked estimation, and the control of smart distribution grids and cyber physical systems in general. He has published more than 200 refereed journal and conference papers. His research interests include statistical signal processing, stochastic modeling, optimization, and control theories. He has served on the editorial board for multiple IEEE journals including the IEEE Transactions on Wireless communications.